

The Dynamics of Large-Amplitude Motion in Energized Molecules

Final Report

for Period July 1, 2011 - January 31, 2016.

David S. Perry

Department of Chemistry  
University of Akron  
Akron, OH 44325-3601

May 2016

Prepared for  
THE U. S. DEPARTMENT OF ENERGY  
AGREEMENT NO. DE-FG02-90ER14151

# The Dynamics of Large-Amplitude Motion in Energized Molecules

## A. Program Scope

Chemical reactions involve large-amplitude nuclear motion along the reaction coordinate that serves to distinguish reactants from products. Some reactions, such as roaming reactions and reactions proceeding through a loose transition state, involve more than one large-amplitude degree of freedom. Because of the limitation of exact quantum nuclear dynamics to small systems, one must, in general, define the active degrees of freedom and separate them in some way from the other degrees of freedom. In this project, we use large-amplitude motion in bound model systems to investigate the coupling of large-amplitude degrees of freedom to other nuclear degrees of freedom [1-15]. This approach allows us to use the precision and power of high-resolution molecular spectroscopy to probe the specific coupling mechanisms involved, and to apply the associated theoretical tools. In addition to slit-jet spectra at the University of Akron [5, 7], the current project period has involved collaboration with Michel Herman and Nathalie Vaeck of the Université Libre de Bruxelles [1, 6, 15], and with Brant Billingham at the Canadian Light Source (CLS) [12]. Recent papers from this project, indicated [ ] are listed in section E.

## B. Recent Progress

### B.1. Vibrational Conical Intersections

A remarkable result from the current grant period is the discovery of systems of  $E \otimes e$  conical intersections between vibrationally adiabatic surfaces in both  $\text{CH}_3\text{OH}$  [12] and  $\text{CH}_3\text{SH}$  (Fig. 1). This discovery leads to a conceptual unity with electronic spectroscopy and provides a new way of thinking about vibrational phenomena. Recently, Hamm and Stock introduced the concept of vibrational conical intersections as a source of ultrafast vibrational relaxation. Exploration of the implications of vibrational conical intersections for vibrational energy transfer and for vibrational spectroscopy is a major thrust of the proposed research for the upcoming grant period.

Conical intersections (CIs) between electronic potential energy surfaces are widespread throughout electronic spectroscopy and are responsible for ultrafast electronic relaxation in diverse circumstances. Whereas these electronic surfaces represent the adiabatic separation of electronic and nuclear motions under the Born-Oppenheimer approximation, it is also possible in some cases to make an (approximate) adiabatic separation of fast and slow vibrational motions. In such cases, the motion of the high frequency vibrations, which might include hydride stretches, can be solved quantum mechanically at each molecular geometry along the low-frequency, large-amplitude torsional or bending coordinates. These slower motions are then solved in the effective potential that is the sum of the electronic potential plus the variation of the high-frequency vibrational energies in the large-amplitude space.

In the electronic context, the 1<sup>st</sup>-order Jahn-Teller effect necessarily results in a CI at the symmetric geometry. Zwanziger and Grant proved that  $E \otimes e$  systems with both 1<sup>st</sup>- and 2<sup>nd</sup>-order Jahn-Teller couplings necessarily have four CIs between the coupled electronic surfaces, one at the  $C_{3v}$  reference geometry and three more at distorted geometries of  $C_s$  symmetry where the magnitudes of the linear and quadratic couplings become equal.

This situation also applies in the purely vibrational context [14], where the adiabatic separation is not between degenerate Born-Oppenheimer electronic states and a degenerate vibrational mode, but now between a high frequency degenerate vibrational state in the electronic ground state and a pair of large-amplitude low-frequency modes [11, 14]. Specifically, we consider the vibronic surfaces (Fig. 1) formed by plotting the energies of the asymmetric CH stretch vibrations as a functions of the torsional angle  $\gamma$  and the CXH bend angle  $\rho$ , where X = O, S. The  $C_{3v}$  reference geometry occurs at  $\rho = 0$  where the CXH group is linear. In this reference geometry, the two asymmetric CH stretch vibrations become

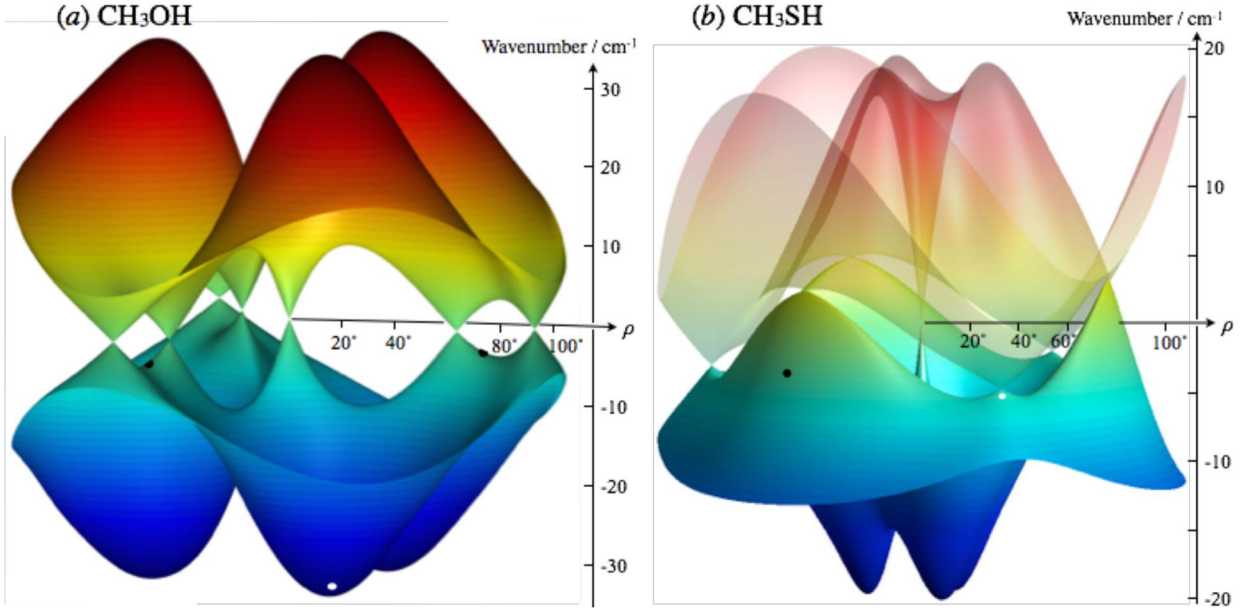


Fig. 1. (a) Relative model frequencies of the two asymmetric CH stretch vibrations ( $\nu_2$  and  $\nu_3$ ) in methanol, represented as surfaces in the 2-dimensional coordinate space of the COH bend angle  $\rho$  and the torsional angle  $\gamma$ . (b) A corresponding plot for methyl mercaptan. The model (Eq. (1)) was fit to *ab initio* frequencies (CCSD(T)/aug-cc-pVTZ) computed at geometries optimized with respect to the other ten internal coordinates. To enhance viewability, the large variations of the average frequency  $V^{0\gamma}$  and of the underlying electronic energy  $U^{m\gamma}$  are suppressed. In (b), the upper surface is rendered partially transparent to make the 7 conical intersections visible. The locations of the global minima in the electronic potential are indicated by white dots, and the torsional saddle points by black dots.

degenerate ( $E$ ), and the large-amplitude coordinates  $\rho$  and  $\gamma$  together become a degenerate CXH bending coordinate ( $e$ ). One significant difference encountered when applying the  $E \otimes e$  formalism to these vibrationally adiabatic surfaces is that the equilibrium geometry is now far from the  $C_{3v}$  reference geometry ( $\rho = 71^\circ$  in CH<sub>3</sub>OH and  $\rho = 83^\circ$  in CH<sub>3</sub>SH) rather than close to it as is typically the case for Jahn-Teller coupling between electronic surfaces. Following Viel and Eisfeld's higher-order treatment of the electronic Jahn-Teller effect,<sup>23</sup> the adiabatic energies of the two asymmetric CH stretches are

$$E_{\pm} = (V^{0\gamma} + U^{0\gamma}) + (V^{3\gamma} + U^{3\gamma}) \cos 3\gamma + (V^{6\gamma} + U^{6\gamma}) \cos 6\gamma \pm \left\{ (W^{1\gamma})^2 + (W^{2\gamma})^2 + (W^{4\gamma})^2 + 2W^{1\gamma}(W^{2\gamma} + W^{4\gamma}) \cos 3\gamma + 2W^{2\gamma}W^{4\gamma} \cos 6\gamma \right\}^{\frac{1}{2}}. \quad (\text{I.1})$$

Here the Fourier parameters  $U^{m\gamma}$  describe the electronic potential, the  $V^{m\gamma}$  describe the diagonal parts of the CH stretch vibrational Hamiltonian, and the  $W^{m\gamma}$  represent the 1<sup>st</sup>- 2<sup>nd</sup>- and 4<sup>th</sup>-order Jahn-Teller couplings. Each of these Fourier parameters is expanded in  $\rho$ . This analytical forms (Fig. 1) fit the *ab initio* data with an RMS error  $< 0.2 \text{ cm}^{-1}$ . Thus classic Jahn-Teller theory provides an excellent description of the global adiabatic behavior of the CH stretch vibrations, providing a beautiful conceptual link between the domains of vibrational and electronic spectroscopy.

Fig. 1 reveals the presence of seven conical intersections in each molecule, one occurring in the  $C_{3v}$  reference geometry ( $\rho = 0^\circ$ ). In methanol, six additional CIs occur in eclipsed conformations ( $C_s$ ) at  $\rho = 62^\circ$  and  $92^\circ$ . The three CI's at  $\rho = 62^\circ$  are close to the torsional saddle point at  $\rho = 71^\circ$ , within the range of the zero-point COH bending amplitude, and therefore accessible to the dynamics at relatively low energies. The pattern is very different in CH<sub>3</sub>SH (Fig. I.1(b)), where CIs occur in both staggered and eclipsed conformations. In CH<sub>3</sub>SH also, the CIs are accessible to the low-energy vibrational dynamics.

## B.2. Six-Fold Internal Rotation

$\text{CH}_3\text{NO}_2$  is a benchmark system for nearly free internal rotation in a 6-fold potential and for the coupling to other small-amplitude vibrations. Since many internal rotor states are populated at room temperature,  $\text{CH}_3\text{NO}_2$  offers an opportunity to study the interaction of these large-amplitude states with the small-amplitude vibrations. Rotationally resolved infrared spectra of  $\text{CH}_3\text{NO}_2$  in the range 400 - 1000  $\text{cm}^{-1}$  have been recorded using Far-infrared Beamline at CLS on a Bruker IFS 125HR spectrometer with 0.001  $\text{cm}^{-1}$  resolution. Together with previous spectra from EMSL at the Pacific Northwest National Laboratory, high-resolution spectra of five bands have been obtained: the in-plane  $\text{NO}_2$  wag (475.2  $\text{cm}^{-1}$ ), the out-of-plane  $\text{NO}_2$  wag (604.9  $\text{cm}^{-1}$ ), NO symmetric bend (657.1  $\text{cm}^{-1}$ ) for CN-stretch and at for CN-stretch (917.2  $\text{cm}^{-1}$ ), and the NO asymmetric stretch (1582.9  $\text{cm}^{-1}$ ). A paper on the 475.2  $\text{cm}^{-1}$  band has appeared [12].

## B.3. Two-Dimensional Large-Amplitude Motion and Coupling to CH Stretches

In molecules with two large-amplitude vibrations (LAV), the LAV's are coupled both to each other and to the other small-amplitude vibrations (SAV) such as CH stretches. Our *ab initio* calculations on  $\text{CH}_3\text{NH}_2$ ,  $\text{CH}_3\text{OH}_2^+$ , and  $\text{CH}_3\text{CH}_2\cdot$  have shown that the couplings connecting the torsion ( $\alpha$ ) and inversion ( $\tau$ ) are very similar across these systems despite the wide variation in the tunneling barriers. In all three cases, the dominant torsion-inversion coupling term is similar, but the coupling of the LAVs to the CH stretches is follows a different pattern in the charged species  $\text{CH}_3\text{OH}_2^+$  than in the other two [13]. The 2-D tunneling patterns in CH stretch excited states are found to vary systematically across the series methanol, methylamine, 2-methylmalonaldehyde and 5-methyltolpolone [5, 8].

## B.4. Intramolecular Dynamics and Quantum Control of Acetylene

The spectroscopic Hamiltonian of acetylene [1] in the normal mode basis contains 155 off-diagonal terms representing four different coupling types (Fig. 2): (i) anharmonic, including Darling-Dennison (DD), (ii) vibrational  $l$ -resonance, (iii) rotational  $l$ -resonance, and (iv) Coriolis [1, 6]. The time-dependent intramolecular vibrational redistribution (IVR) dynamics of acetylene have been computed in unprecedented detail up into the energy range above the onset of new kinds of vibrational motion, such as the local CH stretch, the local bender, and the counter rotator [1]. The results suggest that the search for vinylidene-like states in acetylene spectra will require the preparation of rotationally cold local bender states [4].

The completeness and systematics (Fig. 2) of the acetylene Hamiltonian offer a unique opportunity to test and hone approaches to quantum control. Our first computational results [15] demonstrate the use of optimal control theory to selectively populate dark states in the CH fundamental region. The quantum

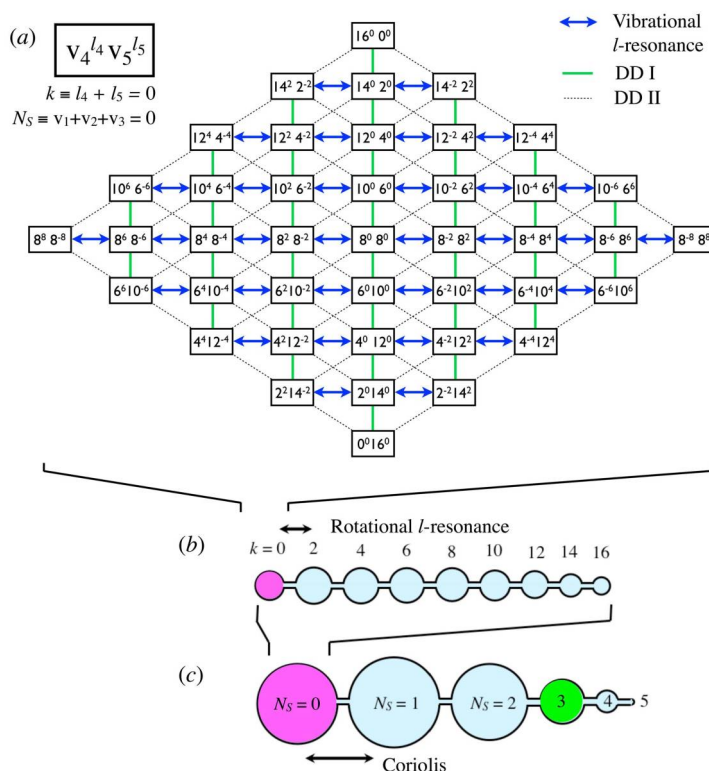


Fig. 2. A schematic of the hierarchical coupling pathways in the acetylene  $\{N_r=16, e g\}$  polyad (897 states).

control part of the project is primarily the work of Nathalie Vaeck and her group in Brussels; our role was provision of the spectroscopic input data and help with the dynamical interpretation.

### C. Statement of Unobligated Balance

There are no funds remaining in this grant.

### D. Project Size and Scope

No significant changes in the project size or scope have occurred within the current funded period nor are such changes planned. The proposed work builds on the success of the current funded period, particularly the discovery of vibrational CIs in methanol and the high-quality CLS spectra of  $\text{CH}_3\text{NO}_2$  and  $\text{CH}_3\text{SH}$ .

### E. Publications from this Project, 2012-2015

- [1] D. S. Perry, J. Martens, B. Amyay, and M. Herman, Hierarchies of Intramolecular Vibration-Rotation Dynamical Processes in Acetylene up to  $13,000\text{ cm}^{-1}$ , *Mol. Phys.* **110**, 2687-2705 (2012). <http://dx.doi.org/10.1080/00268976.2012.711493>.
- [2] R. S. Bhatta, Y. Yimer, M. Tsige, and D. S. Perry, Nonplanar Conformations and Torsional Potentials of Poly(3-hexylthiophene) Oligomers: Density Functional Calculations up to the Dodecamer, *Computational and Theoretical Chemistry* **995**, 36-42 (2012). <http://dx.doi.org/10.1016/j.comptc.2012.06.026>.
- [3] R. S. Bhatta and D. S. Perry, Correlated backbone torsional potentials in poly(3-methylthiophene), *Computational and Theoretical Chemistry* **1008**, 90-95 (2013). <http://dx.doi.org/10.1016/j.comptc.2013.01.003>.
- [4] K. Prozument, R. G. Shaver, M. Ciuba, J. S. Muentner, G. B. Park, J. F. Stanton, H. Guo, B. M. Wong, D. S. Perry, and R. W. Field, A New Approach toward Transition State Spectroscopy, *Faraday Discuss.* **163**, 33-57 (2013). <http://dx.doi.org/10.1039/C3FD20160K>.
- [5] M. B Dawadi, C. M. Lindsay, A. Chirokolava, D. S. Perry and L.-H. Xu, Novel patterns of torsion-inversion-rotation energy levels in the  $\nu_{11}$  asymmetric CH-stretch spectrum of methylamine, *J. Chem. Phys.* **138**, 104305 (2013). <http://dx.doi.org/10.1063/1.4794157>.
- [6] M. Herman and D. S. Perry, Molecular spectroscopy and dynamics: A polyad-based perspective, *Phys. Chem. Chem. Phys.* **15**, 9970-9993 (2013). <http://dx.doi.org/10.1039/C3CP50463H>.
- [7] M. B Dawadi, R. S. Bhatta and D. S Perry, Torsion-Inversion Tunneling Patterns in the CH-Stretch Vibrationally Excited States of the  $G_{12}$  Family of Molecules Including Methylamine, *J. Phys. Chem. A* **117**, 13356-13367 (2013). <http://dx.doi.org/10.1021/jp406668w>.
- [8] R. S. Bhatta, Y. Yimer, D. S. Perry and M. Tsige, Improved force field for molecular modeling of poly(3-hexyl thiophene), *J. Phys. Chem. B* **117**, 10035-10045 (2013). <http://dx.doi.org/10.1021/jp404629a>.
- [9] R. Bhatta, D. Perry and M. Tsige, Nanostructures and Electronic Properties of a High-Efficiency Electron-Donating Polymer, *J. Phys. Chem. A* **117**, 13356-13367 (2013). <http://pubs.acs.org/doi/pdf/10.1021/jp409069d>.
- [10] R. Bhatta, M. Tsige, and D. Perry, Torsionally-induced blue-shift of the band gap in poly(3-hexylthiophene), *J. Comput. Theor. Nanosc.* **11**, 1-8 (2014). <http://dx.doi.org/10.1166/jctn.2014.3621>.
- [11] Mahesh B. Dawadi and David S. Perry, Conical Intersections between Vibrationally Adiabatic Surfaces in Methanol, *J. Chem. Phys.*, **140**, 161101 (2014). <http://dx.doi.org/10.1063/1.4871657>. (featured article)
- [12] Mahesh B. Dawadi, Sylvestre Twagirayezu, David S. Perry and Brant E. Billingham, High-resolution Fourier transform infrared synchrotron spectroscopy of the  $\text{NO}_2$  in-plane rock band of nitromethane, *J. Mol. Spectrosc.* **315**, 10-15 (2015), <http://dx.doi.org/10.1016/j.jms.2014.11.009>.
- [13] Mahesh B. Dawadi, Ram S. Bhatta, David S. Perry, Contrasting patterns of coupling between the CH stretches and the large-amplitude motions in the molecules,  $\text{CH}_3\text{NH}_2$ ,  $\text{CH}_3\text{OH}_2^+$  and  $\text{CH}_3\text{CH}_2^-$ ; *Chem.*

*Phys. Lett.* **624**, 53-58 (2015). (editor's choice) <http://dx.doi.org/10.1016/j.cplett.2015.02.009>.

[14] Bishnu P. Thapaliya, Mahesh B. Dawadi, Christopher Ziegler and David S. Perry, The Vibrational Jahn-Teller Effect in  $E \otimes e$  Systems, *Chem. Phys.*, in press (2015),

<http://dx.doi.org/10.1016/j.chemphys.2015.07.017>.

[15] L. Santos, N. Iacobellis, M. Herman, D.S. Perry, M. Desouter-Lecomte, N. Vaeck, A test of optimal laser impulsion for controlling population within the  $N_s=1$ ,  $N_r=5$  polyad of  $^{12}\text{C}_2\text{H}_2$ , *Mol. Phys., Mol. Phys.*, **113**, 4000-06 (2015), <http://dx.doi.org/10.1080/00268976.2015.1102980>.